

Spectral Risk Measure Minimization in Hazardous Materials Transportation

Liu Su[†] Longsheng Sun[‡] Mark Karwan^ᵇ Changhyun Kwon^{*†}

[†]Department of Industrial and Management Systems Engineering, University of South Florida

[‡]United Airlines

^ᵇDepartment of Industrial and Systems Engineering, University at Buffalo

September 17, 2018

Abstract

Due to catastrophic consequences of potential accidents in hazardous materials (hazmat) transportation, a risk-averse approach for routing is necessary. In this paper, we consider spectral risk measures, for risk-averse hazmat routing, which overcome challenges posed in the existing approaches such as conditional value-at-risk. In spectral risk measures, one can define the spectrum function precisely to reflect the decision maker’s risk preference. We show that spectral risk measures can provide a unified routing framework for popular existing hazmat routing methods based on expected risk, maximum risk, and conditional value-at-risk. We first consider a special class of spectral risk measures, for which the spectrum function is represented as a step function. We develop a mixed integer linear programming model in hazmat routing to minimize these special spectral risk measures and propose an efficient search algorithm to solve the problem. For general classes of spectral risk measures, we suggest approximation methods and path-based approaches. We propose an optimization procedure to approximate general spectrum functions using a step function. We illustrate the usage of spectral risk measures and the proposed computational approaches using data from real road networks.

Keywords: hazardous materials transportation; risk management; spectral risk; coherent risk measures

1 Introduction

The U.S. Occupational Safety and Health Administration (2017) defines hazardous materials (hazmat) as “chemical hazards and toxic substances which pose a wide range of health hazards such as irritation, sensitization, and carcinogenicity and physical hazards such as flammability, corrosion, and explosibility.” Widely used for hazmat transportation are cargo tank trucks. Cargo tank

*Corresponding author: chkwon@usf.edu

trucks transporting with road networks can bring potential risks for the public. According to incident statistics (Pipeline and Hazardous Materials Safety Administration, 2017), there were 3,391 highway transit incidents involving hazmat, causing \$32,806,352 of damages in 2017. In order to protect the road network from severe accidents by hazmat, risk and regulatory analyses have been conducted to provide effective solutions for operations and management in hazmat transportation.

In this paper, we consider a hazmat routing problem to determine a safe path between an origin-destination (OD) pair. Transporting hazmat involves the risk of having an accident, which is often modeled as a discrete random variable (Erkut and Verter, 1998; Erkut and Ingolfsson, 2005). To assess the risk of hazmat transportation, Erkut et al. (2007) identified three key steps including hazard and exposed receptor identification, frequency analysis and consequence modeling and risk calculation. Hazard and exposed receptor identification involves identifying the potential sources, the types, and the quantities of compounds that impact the health and safety on the surrounding environment (Oggero et al., 2006; Yang et al., 2010). In frequency analysis, the probability of an undesirable event, the level of potential receptor exposure and the severity of consequence are considered (Woodruff, 2005; Marhavidas et al., 2011; Rayas and Serrato, 2017). To calculate the risk, all the data related to the relevant area can be collected using GIS (Tomasoni et al., 2010; Van Raemdonck et al., 2013; Torretta et al., 2017). Various models of risk measures for hazmat transport risk are considered in the literature. Most notably, the notion of conditional value-at-risk (CVaR) has been proposed as a risk measure (Toumazis et al., 2013; Toumazis and Kwon, 2016) to provide a flexible routing tool that can incorporate the decision maker’s risk preference. By varying the probability threshold value in the CVaR framework, we can provide routing solutions adequate for risk-neutral to risk-averse decision makers. In addition, Hosseini and Verma (2018) proposed an optimization model for train configuration and routing of rail hazmat shipments with conditional value-at-risk (CVaR).

Basically, CVaR is defined as the “average of the α 100% worst cases in the long tail.” While CVaR exhibits several desirable properties such as coherency in the sense of Artzner et al. (1999), it has a couple of limitations. First, CVaR completely ignores what happens in the dominating $(1 - \alpha)$ 100% cases, by only considering the α 100% worst cases in the long tail; hence, CVaR cannot distinguish random risk variables when their CVaR values are identical. Second, CVaR places a uniform weight in the long tail for the consequences that pass the “cutoff” and, therefore, may fail to provide risk-averseness against extremely large consequences with very small probabilities. Due to these two properties, decision-making based solely on CVaR can lead to less desirable outcomes.

As a way to overcome these limitations, it is natural to consider weighted average of all possible consequences, called the *spectral risk measure* (SRM) (Acerbi, 2002) of the underlying probabilistic risk distribution. The weight function is referred as the spectrum function. Any admissible spectrum function is required to be nonnegative, non-decreasing, and normalized for the spectral risk measure to be coherent. In connection with expected utility theory, researchers suggested some legitimate spectrum functions for constructing spectral risk measures (Dowd et al., 2008; Brandtner, 2016). Spectral risk measures have been studied for financial portfolio optimization problems

(Acerbi and Tasche, 2002; Acerbi, 2004; Acerbi and Simonetti, 2008; Dowd and Blake, 2006) and some researchers (Dowd et al., 2008; Brandtner, 2016) gave guidances on the choice of spectrum functions.

The contributions of this paper can be summarized as follows. For the first time, we introduce SRM as a more general and risk-averse approach in transportation problems, particularly, hazmat routing. We note that some existing hazmat risk measures including CVaR are special cases of SRMs and demonstrate that a weighted sum of those existing hazmat risk measures can be represented as an SRM. Hence, we emphasize that the theory and algorithm developed for SRM minimization can provide a unified framework for hazmat routing in various settings. We also show that SRMs with a special class of discrete spectrum functions can be formulated as the weighted sum of CVaR measures. We devise efficient algorithms for both special and general classes of spectrum functions to find the minimal SRM paths for hazmat routing. We confirm the efficiency of the algorithms and the key advantages of SRM via case studies.

In Section 2 we review various risk measures for hazmat routing and illustrate limitations of the existing CVaR-based approach. After we define the SRM in Section 3, we study a special class of SRMs and propose an efficient algorithm to solve the SRM minimization model in Section 4. For general spectral risk measures, we propose an approximation scheme to simplify the problem in Section 5. Case studies of road networks are conducted and comparisons for different hazmat routing models are introduced in Section 6. Section 7 provides concluding remarks for this paper.

2 Review of Risk Measures for Hazmat Routing

For a graph $G(\mathcal{N}, \mathcal{A})$, we denote the accident probability and the accident consequence in arc $(i, j) \in \mathcal{A}$ by p_{ij} and c_{ij} , respectively. To transport a commodity, the approximated risk distribution along path l can be written as follows (Jin and Batta, 1997):

$$\Pr[R^l = x] \approx \begin{cases} 1 - \sum_{(i,j) \in \mathcal{A}^l} p_{ij} & \text{if } x = 0 \\ p_{ij} & \text{if } x = c_{ij} \text{ for some } (i, j) \in \mathcal{A}^l \end{cases} \quad (1)$$

Note that the approximation is from the fact that $p_{ij} \ll 1$ for hazmat accidents, and therefore, $p_{ij}p_{i'j'} \approx 0$ for any $(i, j), (i', j') \in \mathcal{A}$. The accident consequence (loss) in path l can be written as the following distribution (Kang et al., 2014a):

$$R^l = \begin{cases} 0, & \text{w.p. } 1 - \sum_{i=1}^{|\mathcal{A}^l|} p_{(i)}^l \\ c_{(1)}^l, & \text{w.p. } p_{(1)}^l \\ \vdots \\ c_{(|\mathcal{A}^l|)}^l, & \text{w.p. } p_{(|\mathcal{A}^l|)}^l \end{cases} \quad (2)$$

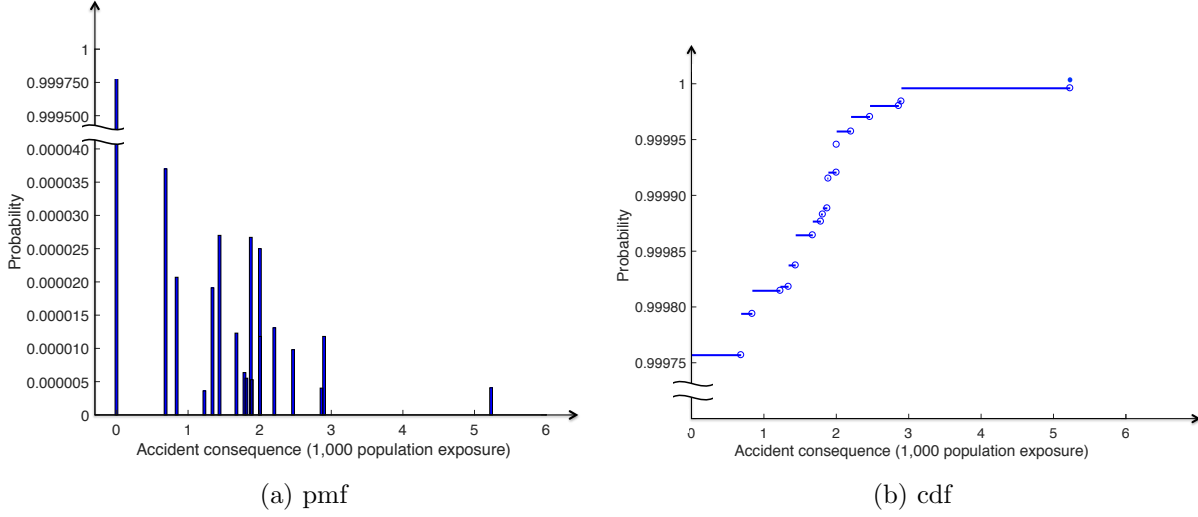


Figure 1: The pmf and cdf for the accident consequence of a path

where \mathcal{A}^l is the set of arcs contained in path l , $c_{(i)}^l$ is the i -th smallest in the set $\{c_{ij} : (i, j) \in \mathcal{A}^l\}$, and $p_{(i)}^l$ is the probability corresponding to $c_{(i)}^l$. The probability mass function (pmf) and cumulative distribution function (cdf) for R^l of a path in the Ravenna network¹ is shown in Figure 1. Note that the accident probabilities are as small as 10^{-5} .

For the random risk variable R^l , several measures of risk have been proposed in the literature, as summarized in Table 1. Let us consider two risk measures that are popular in the literature: the traditional risk (TR) and the maximum risk (MM). The TR is the expected consequence along a path, and the MM is the maximum arc consequence in a path. Both measures invoke some problems in hazmat transportation. First, the TR measure considers the expected value, which is risk-neutral. In hazmat transportation, it is recommended to use risk-averse approaches to avoid catastrophic consequences. On the other hand, the MM measure, although risk-averse, often leads to a circuitous path (Erkut and Ingolfsson, 2005).

2.1 VaR and CVaR Defined

As a flexible alternative that covers risk attitudes between the attitudes of TR and MM, the notion of value-at-risk (VaR) and conditional value-at-risk (CVaR) have been proposed. VaR and CVaR are defined as follows:

Definition 1 (VaR Measure). *The value-at-risk (VaR) along path l is defined as follows:*

$$\text{VaR}_p^l = \inf\{x : \Pr[R^l \leq x] \geq p\} \quad (3)$$

where $p \in (0, 1)$ is a threshold probability.

¹The path is $106 \rightarrow 1 \rightarrow 2 \rightarrow 7 \rightarrow 17 \rightarrow 19 \rightarrow 28 \rightarrow 34 \rightarrow 39 \rightarrow 47 \rightarrow 55 \rightarrow 52 \rightarrow 53 \rightarrow 48 \rightarrow 51 \rightarrow 63 \rightarrow 67 \rightarrow 71$, and the details about the Ravenna network (Bonvicini and Spadoni, 2008; Erkut and Gzara, 2008) are introduced in Section 6.

Table 1: Measures of hazmat transport risk along path l . $\mathbb{E}[R^l]$ and $\mathbb{V}\mathbb{A}\mathbb{R}[R^l]$ denote the expected value and the variance of random risk R^l in path l , respectively. Note that q , k , p , and α are some model-specific scalars.

| Model | Risk Measure | |
|-----------------------------------|---|--|
| Expected Risk ¹ | $\text{TR}^l = \mathbb{E}[R^l]$ | $\approx \sum_{(i,j) \in \mathcal{A}^l} p_{ij} c_{ij}$ |
| Population Exposure ² | PE^l | $= \sum_{(i,j) \in \mathcal{A}^l} c_{ij}$ |
| Incident Probability ³ | $\text{IP}^l = \Pr[R^l > 0]$ | $\approx \sum_{(i,j) \in \mathcal{A}^l} p_{ij}$ |
| Perceived Risk ⁴ | $\text{PR}^l = \mathbb{E}[(R^l)^q]$ | $\approx \sum_{(i,j) \in \mathcal{A}^l} p_{ij} (c_{ij})^q$ |
| Maximum Risk ⁵ | $\text{MM}^l = \sup R^l$ | $= \max_{(i,j) \in \mathcal{A}^l} c_{ij}$ |
| Mean-Variance ⁵ | $\text{MV}^l = \mathbb{E}[R^l] + k\mathbb{V}\mathbb{A}\mathbb{R}[R^l]$ | $\approx \sum_{(i,j) \in \mathcal{A}^l} (p_{ij} c_{ij} + k p_{ij} (c_{ij})^2)$ |
| Disutility ⁵ | $\text{DU}^l = \mathbb{E}[\exp(kR^l)]$ | $\approx \sum_{(i,j) \in \mathcal{A}^l} p_{ij} [\exp(kc_{ij}) - 1]$ |
| Conditional Risk ⁶ | $\text{CR}^l = \mathbb{E}[R^l R^l > 0]$ | $\approx \left(\sum_{(i,j) \in \mathcal{A}^l} p_{ij} c_{ij} \right) / \left(\sum_{(i,j) \in \mathcal{A}^l} p_{ij} \right)$ |
| Value-at-Risk ⁷ | $\text{VaR}_p^l = \inf \{x : \Pr[R^l \leq x] \geq p\}$ | |
| Conditional VaR ⁸ | $\text{CVaR}_\alpha^l = \frac{1}{1-\alpha} \int_\alpha^1 \text{VaR}_p^l dp$ | $\approx \min_r \left(r + \frac{1}{1-\alpha} \sum_{(i,j) \in \mathcal{A}^l} p_{ij} [c_{ij} - r]^+ \right)$ |

¹ Alp (1995); ² ReVelle et al. (1991); ³ Saccomanno and Chan (1985); ⁴ Abkowitz et al. (1992); ⁵ Erkut and Ingolfsson (2000); ⁶ Sivakumar et al. (1993); ⁷ Kang et al. (2014b); ⁸ Toumazis et al. (2013)

Definition 2 (CVaR Measure). *The conditional value-at-risk (CVaR) along path l is defined as follows:*

$$\text{CVaR}_\alpha^l = \frac{1}{1-\alpha} \int_\alpha^1 \text{VaR}_p^l dp \quad (4)$$

for a threshold probability $\alpha \in (0, 1)$.

In the context of hazmat transportation, VaR and CVaR, with a threshold probability α , become identical to TR when α is sufficiently small, and identical to MM when α is sufficiently large (Toumazis et al., 2013). Therefore, VaR and CVaR in hazmat transportation provide risk measures that are more general than both the TR and MM measures.

Artzner et al. (1999) propose the four axioms for any risk measure ξ , which maps a random loss X to a real number, to be *coherent*:

Translation Invariance For any real number m , $\xi(X + m) = \xi(X) + m$.

Subadditivity For all X_1 and X_2 , $\xi(X_1 + X_2) \leq \xi(X_1) + \xi(X_2)$.

Positive Homogeneity For all $\lambda \geq 0$, $\xi(\lambda X) = \lambda \xi(X)$.

Monotonicity For all X_1 and X_2 with $X_1 \leq X_2$ a.s., $\xi(X_1) \leq \xi(X_2)$.

Not all risk measures in Table 1 are coherent. Most notably, VaR is not a coherent risk measure, while CVaR is coherent (Rockafellar and Uryasev, 2002).

2.2 Limitation of CVaR: an Illustrative Example

While CVaR provides a flexible and coherent risk measure for hazmat routing to avoid high consequence events, it has a limitation. For the demonstration purpose, let us consider the following three discrete random variables:

$$R^1 = \begin{cases} 0 & \text{w.p. } 0.900 \\ 5 & \text{w.p. } 0.090 \\ 10 & \text{w.p. } 0.008 \\ 50 & \text{w.p. } 0.002 \end{cases}, \quad R^2 = \begin{cases} 0 & \text{w.p. } 0.900 \\ 5 & \text{w.p. } 0.090 \\ 18 & \text{w.p. } 0.010 \end{cases}, \quad R^3 = \begin{cases} 0 & \text{w.p. } 0.900 \\ 10 & \text{w.p. } 0.090 \\ 18 & \text{w.p. } 0.010 \end{cases}. \quad (5)$$

CVaR measures for the above three random (loss) variables with various probability threshold values can be computed as follows (Rockafellar and Uryasev, 2002; Pflug, 2000):

$$\text{CVaR}_\alpha^i = \min_r \left\{ r + \frac{1}{1-\alpha} \mathbb{E}[R^i - r]^+ \right\}$$

for each $i = 1, 2, 3$ where $[x]^+ = \max\{0, x\}$. We obtain the following values:

| α | CVaR_α^1 | CVaR_α^2 | CVaR_α^3 |
|----------|------------------------|------------------------|------------------------|
| 0.900 | 6.3 | 6.3 | 10.8 |
| 0.990 | 18.0 | 18.0 | 18.0 |
| 0.998 | 50.0 | 18.0 | 18.0 |

From the above, it is obvious that R^2 is the most desirable, since it is a non-dominated solution for all probability thresholds. It is, however, not straightforward to make R^2 outstanding using CVaR. When R^1 , R^2 , and R^3 are compared at $\alpha = 0.990$, both have the identical CVaR value, and hence CVaR-based decision making is indifferent among the three random variables. We note, however, that R^1 has a significant loss of 50 with probability 0.002, which should be avoided. To distinguish R^1 from R^2 , increasing α to 0.998 does not help, because it will still remain indifferent between R^2 and R^3 . Although R^3 exhibits the same long-tail behavior as R^2 does, R^3 certainly has a higher CVaR value than R^2 when $\alpha = 0.900$; hence R^2 should be preferred to R^3 . As a remedy, one can consider a weighted sum as follows:

$$WS^l = w_1 \text{CVaR}_{0.900}^l + w_2 \text{CVaR}_{0.990}^l + w_3 \text{CVaR}_{0.998}^l,$$

which surely confirms R^2 as the least risky choice for any positive weight parameters w_1 , w_2 , and w_3 . For risk-aversion, it is desirable to have $w_1 < w_2 < w_3$. Note that WS^l may or may not be a coherent risk measure depending on how the weight parameters are chosen. This motivates us to consider another class of coherent risk measures that are more general than CVaR.

3 Defining the Spectral Risk Measure

To extend and generalize the notion of CVaR, we define the spectral risk measure—a coherent risk measure first introduced by Acerbi (2002).

Definition 3 (Spectral Risk Measure). *The spectral risk measure (SRM) for hazmat routing risk along path l is defined as follows:*

$$\text{SRM}_\phi^l = \int_0^1 \phi(p) \text{VaR}_p^l \, dp \tag{6}$$

where $\phi : [0, 1] \rightarrow \mathbb{R}_+$ is a nonnegative and non-decreasing function such that

$$\int_0^1 \phi(p) \, dp = 1. \tag{7}$$

Note that (7) is necessary for the translational invariance condition (Acerbi, 2004).

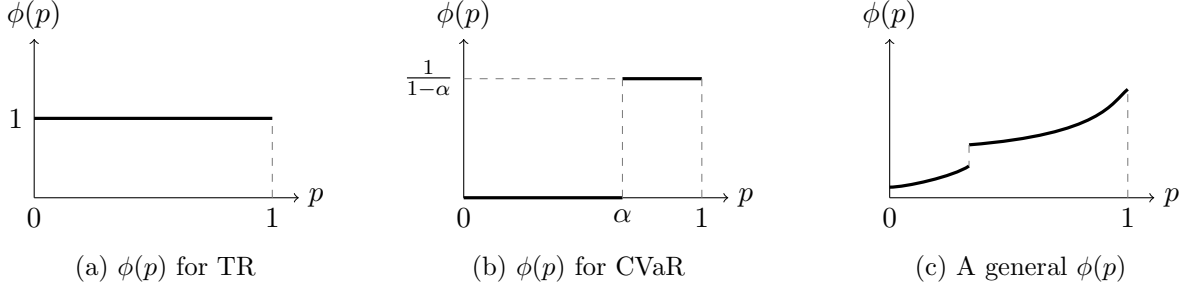


Figure 2: Example spectrum functions

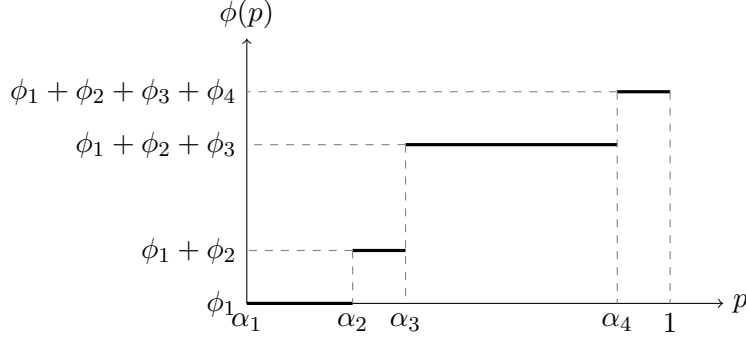


Figure 3: An example of the spectral risk measure (8) with $n = 4$

We can easily see that CVaR is a special case of spectral risk measures, by noting that

$$\phi(p) = \begin{cases} 1/(1 - \alpha) & \text{if } p > \alpha \\ 0 & \text{if } p \leq \alpha \end{cases}$$

for a certain probability $\alpha \in (0, 1)$. Since TR and MM are the same as CVaR when α is very small and large, respectively (Toumazis et al., 2013; Toumazis and Kwon, 2016), TR and MM are also special cases of spectral risk measures. The comparisons can be seen in Figure 2. It is illustrated that TR covers full probability spectrum $[0, 1]$ uniformly, while CVaR covers only $[\alpha, 1]$ uniformly. A general spectrum function $\phi(p)$ may be defined to cover the full probability spectrum $[0, 1]$, but non-uniformly.

4 A Class of Spectral Risk Measures Applied in Hazmat Transportation

In this section, we consider a special class of spectrum functions; namely, non-decreasing step functions. We show that the spectral risk measure defined by such spectrum functions can be represented as a weighted sum of CVaR measures.

Let us consider a spectrum function ϕ that is a non-decreasing, step function. In particular, we

consider

$$\phi(p) = \begin{cases} \phi_1, & \forall p \in (\alpha_1, \alpha_2] \\ \phi_1 + \phi_2, & \forall p \in (\alpha_2, \alpha_3] \\ \phi_1 + \phi_2 + \phi_3, & \forall p \in (\alpha_3, \alpha_4] \\ \vdots \\ \phi_1 + \phi_2 + \dots + \phi_n, & \forall p \in (\alpha_n, 1) \end{cases} \quad (8)$$

where the values of ϕ_k are nonnegative constants and $\alpha_1 = 0$. An example of such ϕ is provided in Figure 3 when $n = 4$.

Lemma 1 (Normalization). *For a step function (8), the values of ϕ_k must satisfy $\sum_{k=1}^n \phi_k(1-\alpha_k) = 1$.*

When the spectrum function of the form (8) is used, the spectral risk measure can be simplified as a weighted sum of CVaR measures.

Theorem 1. *With (8), the spectral risk measure for path l with spectrum function ϕ can be written as follows:*

$$\text{SRM}_\phi^l = \sum_{k=1}^n \phi_k(1-\alpha_k)\text{CVaR}_{\alpha_k}^l \quad (9)$$

where

$$\text{CVaR}_{\alpha_k}^l = \min_{r_k} \left[r_k + \frac{1}{1-\alpha_k} \sum_{(i,j) \in \mathcal{A}^l} p_{ij} [c_{ij} - r_k]^+ \right] \quad (10)$$

for all $k = 1, \dots, n$.

As a corollary, Theorem 2 demonstrates how to construct a weighted sum of TR, CVaR, and MM, while maintaining coherency, as a special case of SRM.

Theorem 2. *Consider a weighted sum of TR, CVaR with α , and MM for path $l \in \mathcal{P}$ as follows:*

$$\Sigma^l = w_1 \text{TR}^l + w_2 \text{CVaR}_\alpha^l + w_3 \text{MM}^l \quad (11)$$

where $w_1, w_2, w_3 \geq 0$ and $\alpha \in (0, 1)$. Let p^l be a constant such that $\Pr[R^l = \max_{(i,j) \in \mathcal{A}^l} c_{ij}] < p^l < 1$ and $\alpha < p^l$. If $w_1 + w_2(1-\alpha) + w_3(1-p^l) = 1$, then the weighted sum Σ^l itself is an SRM.

4.1 Spectral Risk Measure Minimization

The routing problem based on the spectral risk measure is to choose a path $l \in \mathcal{P}$ that minimizes the spectral risk measure from an origin to a destination; that is,

$$\min_{l \in \mathcal{P}} \text{SRM}_\phi^l. \quad (12)$$

Note that (12) is a path-based formulation for hazmat transportation, which requires path enumeration. Instead of the path-based formulation, we present an arc-based formulation that can

represent all feasible paths implicitly using flow conservation constraints. Let us define:

$$\Omega \equiv \left\{ x : \sum_{(i,j) \in \mathcal{A}} x_{ij} - \sum_{(j,i) \in \mathcal{A}} x_{ji} = b_i \quad \forall i \in \mathcal{N}, \text{ and } x_{ij} \in \{0,1\} \quad \forall (i,j) \in \mathcal{A} \right\}$$

where the parameter b_i has the following values:

$$b_i = \begin{cases} 1 & \text{if } i = \text{origin} \\ -1 & \text{if } i = \text{destination} \\ 0 & \text{otherwise} \end{cases}$$

We obtain the following results:

Theorem 3. *The hazmat routing problem with SRM (12) is equivalent to:*

$$\min_{l \in \mathcal{P}} \text{SRM}_{\phi}^l = \min_r \left[\sum_{k=1}^n \phi_k (1 - \alpha_k) r_k + z(r) \right] \quad (13)$$

where $z(r)$ is obtained by a shortest path problem

$$z(r) = \min_{x \in \Omega} \sum_{(i,j) \in \mathcal{A}} \left\{ \sum_{k=1}^n \phi_k p_{ij} [c_{ij} - r_k]^+ \right\} x_{ij} \quad (14)$$

and $r = [r_1, \dots, r_n]^{\top} \in \mathbb{R}^n$.

With Theorem 3, we can solve the routing problem (12) by searching the space of r . With each search of r , we can obtain the path and its spectral risk measure value by solving a shortest-path problem (14). It is, however, inefficient to search r within \mathbb{R}^n when the dimension n is large. We provide useful results to reduce the searching efforts for r .

Lemma 2 (Kang et al. 2014a). *For any $\alpha \in (0, 1)$, we have $\text{VaR}_{\alpha}^l \in \{0\} \cup \{c_{ij} : (i, j) \in \mathcal{A}\}$.*

Lemma 3. *For all $0 < \alpha_1 < \alpha_2 < 1$, there exist minimizers $r^{\alpha_1} = \text{VaR}_{\alpha_1}^l$ and $r^{\alpha_2} = \text{VaR}_{\alpha_2}^l$ of $F_{\alpha_2}^l(r)$ and $F_{\alpha_2}^l(r)$, respectively, such that $r^{\alpha_1} \leq r^{\alpha_2}$ where*

$$F_{\alpha}^l(r) = r + \frac{1}{1 - \alpha} \sum_{(i,j) \in \mathcal{A}^l} p_{ij} [c_{ij} - r]^+$$

Therefore we only need to search for $r \in \{0\} \cup \{c_{ij} : (i, j) \in \mathcal{A}\}$ to obtain CVaR_{α}^l . For solving the SRM minimization problem (13), Lemma 2 says that it is sufficient to search the mesh determined by 0 and c_{ij} only, and the number of searches is $(|\mathcal{A}| + 1)^n$. In addition, Lemma 3 indicates that there is no need to search any r such that $r_k > r_{k+1}$ for any k .

The computational method inspired by Lemmas 2 and 3 searches all valid combinations thus guaranteeing an exact optimal solution. In addition, we can also consider a mixed integer linear

programming (MILP) reformulation of (13) after linearization, and use an optimization solver for a solution.

4.2 MILP Reformulation

The SRM minimization model (13) can be reformulated as a mixed integer linear programming (MILP) problem. We introduce new continuous variables y_{ijk} . When x_{ij} are binary, we observe

$$y_{ijk} = [c_{ij} - r_k]^+ x_{ij} = \max\{c_{ij} - r_k, 0\} x_{ij} = \max\{c_{ij} x_{ij} - r_k, 0\}.$$

Therefore, we obtain the following equivalent formulation:

$$\min_{l \in \mathcal{P}} \text{SRM}_\phi^l = \min_{r, x, y} \left[\sum_{k=1}^n \phi_k (1 - \alpha_k) r_k + \sum_{(i,j) \in \mathcal{A}} \sum_{k=1}^n \phi_k p_{ij} y_{ijk} \right] \quad (15)$$

subject to

$$\begin{aligned} x &\in \Omega \\ x_{ij} &\in \{0, 1\} && \forall (i, j) \in \mathcal{A} \\ y_{ijk} &\geq c_{ij} x_{ij} - r_k && \forall (i, j) \in \mathcal{A}, k = 1, \dots, n \\ y_{ijk} &\geq 0 && \forall (i, j) \in \mathcal{A}, k = 1, \dots, n. \end{aligned}$$

The computational time for both approaches—the exact search method based on Lemmas 2 and 3 and any exact algorithms for solving the MILP problem (15)—increases exponentially as n increases.

4.3 A Multi-dimensional Cyclic Coordinate Search Method with Mapping

We propose a heuristic search algorithm to find a quality solution more efficiently. The algorithm still utilizes the results from Lemmas 2 and 3 but we only need to evaluate a very limited number of combinations of $\{0\} \cup \{c_{ij} : (i, j) \in \mathcal{A}\}$ values in ascending order of r . It is a modification of the multi-dimensional cyclic coordinate search algorithm by mapping the infeasible points to the feasible region. For each dimension, we use a line search method. The algorithm is summarized in Algorithm 1.

The definition of $z(r)$ is provided in (14) and the function value can be obtained by solving a shortest path problem for any given r value. To find the minimum on each dimension in Step 2, we solve the shortest path problem only when the first component of the objective $\sum_{k=1}^n \phi_k (1 - \alpha_k) r_k^t$ is smaller than the current best minimum. Furthermore, we can utilize a line search algorithm such as golden section search on all the values in $\{0\} \cup \{c_{ij} : (i, j) \in \mathcal{A}\}$ to speed up the solution process. The above algorithm obtains the minimum value by searching each dimension sequentially, while enforcing the ascending order of r . This is realized by mapping a search point to the diagonal direction when it surpasses the diagonal line. Since this algorithm does not guarantee the global

Algorithm 1 A Multi-dimensional Cyclic Coordinate Search Method with Mapping for A Class of SRM Hazmat Routing Problems

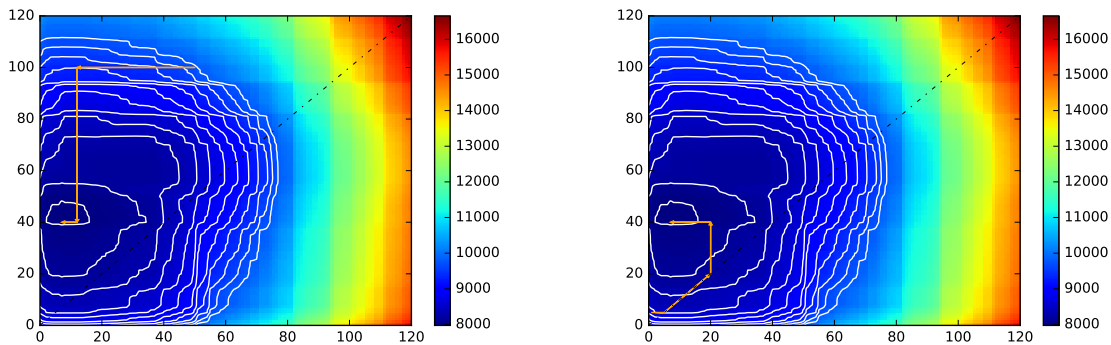
- 1: Let $Z = +\infty$. Sample an initial solution r^0 uniformly from $\{0\} \cup \{c_{ij} : (i, j) \in \mathcal{A}\}$ and sort in ascending order. Let $r^c = r^0$, $r^l = r^0$.
- 2: Let $k = 1$ and go to Step 3.
- 3: Find the value $\lambda_k \in \{0\} \cup \{c_{ij} : (i, j) \in \mathcal{A}\}$ such that the objective $z(r^t)$ is minimized where

$$r_m^t = \begin{cases} r_m^c, & \text{if } r_m^c < \lambda_k, m < k \text{ or } r_m^c > \lambda_k, m > k \\ \lambda_k, & \text{otherwise,} \end{cases} \quad \forall m = 1, \dots, n.$$

Let $r^c = r^t$ and go to Step 4.

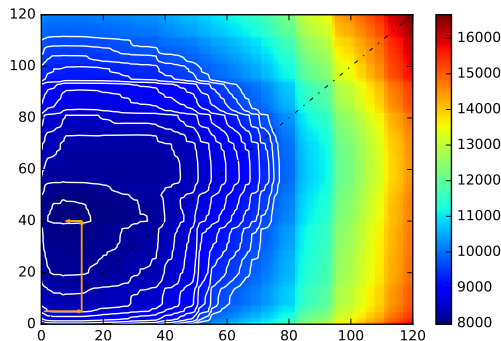
- 4: If $k < n$, let $k = k + 1$ and go to Step 3; otherwise go to Step 5.
 - 5: If r^c equals r^l , let $Z = \sum_{k=1}^n \phi_k(1 - \alpha_k)r_k^c + z(r^c)$ and terminate. Otherwise, let $r^l = r^c$ and go to Step 2.
-

optimality, we may begin with multiple initial points to ensure the quality of the final solution.



(a) without diagonal direction

(b) with diagonal direction



(c) without enforcing ascending order of r

Figure 4: Search processes

Examples of the search process for OD pair (1,84) in the Buffalo network (Toumazis and

Kwon, 2016) with two dimensions are shown in Figure 4. In this example, we used $n = 3$, $\alpha_2 = 0.999970$, $\alpha_3 = 0.999985$, and $\phi_1 = 0, \phi_2 = 22222.22, \phi_3 = 22222.22$. Figure 4a shows the algorithm process without hitting the diagonal line while Figure 4b demonstrates one with searching the direction on the diagonal line. For the same starting point as in Figure 4b, Figure 4c shows the search process with a traditional multi-dimensional cyclic search without enforcing the ascending order of r . By comparing Figures 4b and 4c, we can see how the points that surpass the diagonal line are mapped. While both algorithms reach the same optimal solution in this example, we also have found some examples that can obtain worse solutions in higher dimensions without enforcing an ascending order of r . In general, enforcing an ascending order of r helps finding an optimal solution.

5 General Spectral Risk Measures Applied in Hazmat Transportation

In this section, we consider the spectral risk measures with any general spectrum function. For any integrable, non-decreasing spectrum function $\phi(\cdot)$ that satisfies the normalization condition (7), we can define the general spectral risk measure of path l based on Definition 3. While the general spectrum function can be continuous, the underlying random risk variable in hazmat transportation is still discrete as shown in (2).

The general SRM minimization model in hazmat transportation is represented as follows:

$$\begin{aligned}
\min_{l \in \mathcal{P}} \text{SRM}_\phi^l &= \int_0^1 \phi(p) \text{VaR}_p^l \, dp \\
&= \sum_{k=0}^{|\mathcal{A}^l|} \int_{\pi_{(k)}^l}^{\pi_{(k+1)}^l} \phi(p) c_{(k)}^l \, dp \\
&= \sum_{k=0}^{|\mathcal{A}^l|} \phi_{(k)}^l c_{(k)}^l
\end{aligned} \tag{16}$$

where

$$\pi_{(k)}^l = \begin{cases} 0, & \text{if } k = 0 \\ 1 - \sum_{i=k}^{|\mathcal{A}^l|} p_{(i)} & \text{if } k = 1, 2, \dots, |\mathcal{A}^l| \\ 1, & \text{if } k = |\mathcal{A}^l| + 1 \end{cases}$$

$$\phi_{(k)}^l = \int_{\pi_{(k)}^l}^{\pi_{(k+1)}^l} \phi(p) \, dp$$

and $c_{(0)}^l = 0$. Different from the case with step spectrum functions, the general SRM minimization problem does not allow a transformation into an arc-based formulation.

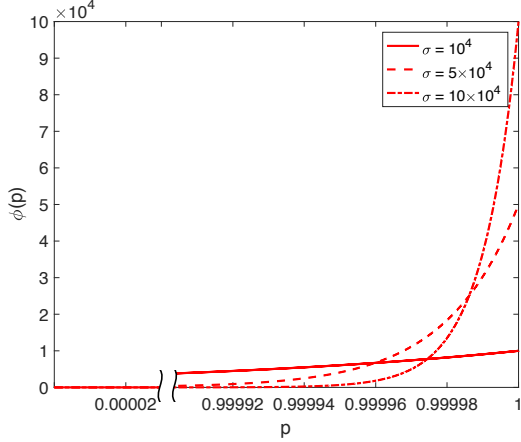


Figure 5: Exponential Spectrum functions

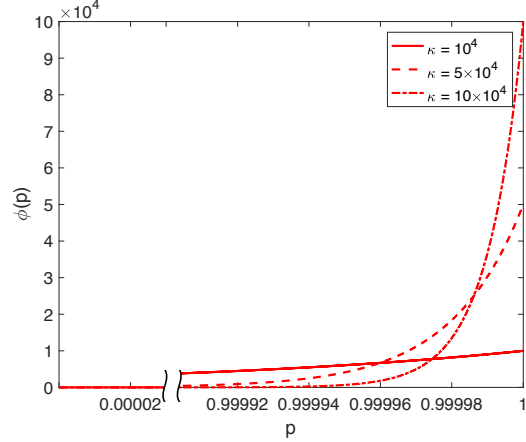


Figure 6: Power Spectrum functions

5.1 Exponential and Power Spectral Risk Measures

We introduce possible choices for the spectrum function $\phi(\cdot)$. Inspired by popular utility functions from expected utility theory, Dowd et al. (2008) proposed the following spectrum functions:

$$\begin{array}{ll} \text{exponential functions} & \phi(p) = \frac{\sigma e^{-\sigma(1-p)}}{1 - e^{-\sigma}}, \sigma > 0 \end{array} \quad (17)$$

$$\begin{array}{ll} \text{power functions} & \phi(p) = \kappa p^{\kappa-1}, \kappa \geq 1 \end{array} \quad (18)$$

In fact, Dowd et al. (2008) proposed another class of power functions, which creates some inconsistencies between the risk measure value and the risk-aversion level of decision makers. Hence, we only consider (17) and (18). Figures 5 and 6 show the exponential and power spectrum functions with some parameters. Power functions exhibit similar properties as exponential functions if parameters are large.

Wächter and Mazzoni (2013) concluded that the inconsistencies found in Dowd et al. (2008) arise because of an inappropriate construction of the link between utility functions and the risk spectrum. Recently, Brandtner and Kürsten (2017) proposed procedures to develop spectrum functions with which spectral risk and expected utility users can have the same decisions. The linking procedure to produce spectrum functions, however, requires knowledge of the risk distribution beforehand. In this paper, the risk distribution is dependent on the path choice of hazmat transportation. Therefore, the linking approach cannot be applied to our work.

In hazmat transportation, the distribution of risk is highly skewed to the right due to extremely small probabilities for accidents. If we use small σ and κ in spectral risk measures, it addresses very limited weights for catastrophic accident consequences thus having similar results to TR. To develop appropriate spectral risk measures reflecting a risk-averse attitude towards hazmat transportation, large parameters for exponential functions and power functions are used.

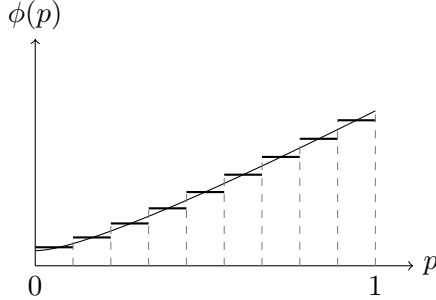


Figure 7: Approximating a general spectrum function by a step function

5.2 Computational Methods for the General Cases

The general SRM minimization problem (16) cannot be transformed into an arc-based formulation. While we can solve the problem directly based on the path-based formulation in (16), the path-based formulation requires path enumeration beforehand. Once we prepare a set of feasible paths, the spectral risk measure SRM_ϕ^l in (16) can be computed for each path l from the set. While full path enumeration guarantees optimality of the solution obtained, it costs enormous computational effort as the number of available paths between an OD pair increases exponentially. A possible method in such a case is to limit the problem to a set of geographically dissimilar paths (Akgün et al., 2000; Kang et al., 2014a) and choose a path from those dissimilar paths.

Another approach is to approximate the general spectrum function $\phi(\cdot)$ by a step function of the form in (8) and solve the corresponding SRM minimization problem as discussed in Section 4. Figure 7 demonstrates an example. We can use Algorithm 1 in Section 4.3 to solve such approximated problems. To approximate $\phi(\cdot)$ accurately, however, we require a large number of steps. Such an approximation is inefficient for large-scale problems, since the dimension of the search space increases exponentially and we need to solve many shortest-path problems.

We can also combine the two ideas. The approximation based on a step function determines probability breakpoints α_k for $k = 1, \dots, n$ and corresponding CVaR measures $\text{CVaR}_{\alpha_k}^l$ for path l . For each k , we can find the minimal CVaR path, which can be done by solving a series of shortest-path problems. For the solution procedure for finding the minimal CVaR path, see Toumazis et al. (2013); it is a single-dimensional special case of Algorithm 1. By collecting the minimal CVaR paths, we can form a set of paths for the given OD pair. The spectral risk measure (16) can be computed for each path in the set, thus determining the minimal SRM path. We summarize the two methods based on approximation in Algorithms 2 and 3.

Algorithm 2 A Multi-dimensional Cyclic Coordinate Search Method with Mapping for General SRM Hazmat Routing Problems

- 1: Approximate the given spectrum function $\phi(\cdot)$ using a step function and obtain $\alpha_1, \dots, \alpha_n$ and ϕ_1, \dots, ϕ_n .
 - 2: Solve the corresponding minimization problem using Algorithm 1 in Section 4.3.
-

Algorithm 3 A CVaR Path Generation Method for General SRM Hazmat Routing Problems

- 1: Approximate the given spectrum function $\phi(\cdot)$ using a step function and obtain $\alpha_1, \dots, \alpha_n$ and ϕ_1, \dots, ϕ_n .
- 2: For each $k = 1, \dots, n$, solve

$$\min_{l \in \mathcal{P}} \text{CVaR}_{\alpha_k}$$

using the method in Toumazis et al. (2013), and call the obtained path l_k .

- 3: Compute $\text{SRM}_{\phi}^{l_k}$ in (16) for each $k = 1, \dots, n$ and choose the path with the minimal value.
-

Although we consider a limited number of paths, Algorithm 3 is expected to produce optimal or near-optimal solutions, since minimal CVaR paths can be regarded as safe paths already and hence are good candidates for the minimal SRM path. Furthermore, the value of n in Algorithm 3 can be made much larger than in Algorithm 2. While the computational complexity in Algorithm 1 used by Algorithm 2 increases exponentially as n increases, it increases linearly in Algorithm 3.

5.3 Optimal Approximation by Step Functions

We propose an optimization procedure to approximate the general spectrum function by a step function. Suppose we use n number of probability breakpoints $\alpha_1, \dots, \alpha_n$. In each interval $[\alpha_{k-1}, \alpha_k]$, we approximate $\phi(\cdot)$ by a constant h_k , as shown in Figure 8. To minimize the approximation error, we formulate an optimization problem as follows:

$$\min E(\alpha, h) = \sum_{k=1}^n \int_{\alpha_{k-1}}^{\alpha_k} (\phi(p) - h_k)^2 dp \quad (19)$$

$$\text{s.t. } \sum_{k=1}^n h_k (\alpha_k - \alpha_{k-1}) = 1 \quad (20)$$

$$\alpha_{k-1} \leq \alpha_k, k = 1, \dots, n. \quad (21)$$

where α_0 is set to zero. To make it consistent with the notation in Section 4, we can let $h_k = \sum_{s=1}^k \phi_s$ or $h_k - h_{k-1} = \phi_k$ with $\alpha_0 = 0$ and $\alpha_n = 1$. Problem (19) minimizes the sum of the squared approximation errors, while enforcing the normalization condition (7) in constraint (20).

As done similarly in Maybee et al. (1979), we obtain the following result:

Theorem 4. *The optimal approximation problem (19) is equivalent to the following unconstrained optimization problem:*

$$\min J(\alpha) = - \sum_{k=1}^n \frac{[\Phi(\alpha_k) - \Phi(\alpha_{k-1})]^2}{\alpha_k - \alpha_{k-1}} \quad (22)$$

where $\Phi(\alpha_k) = \int_0^{\alpha_k} \phi(p) dp$. Once optimal α_k values are determined, we can determine

$$h_k = \frac{\Phi(\alpha_k) - \Phi(\alpha_{k-1})}{\alpha_k - \alpha_{k-1}} \quad (23)$$

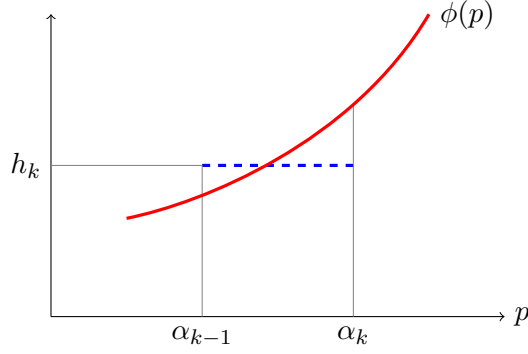


Figure 8: Approximating $\phi(p)$ by h_k in the interval of $[\alpha_{k-1}, \alpha_k]$.

for all $k = 1, \dots, n$.

To minimize $J(\alpha)$, a gradient projection algorithm is implemented. Note that $\frac{\partial \Phi(\alpha_k)}{\partial \alpha_k} = \phi(\alpha_k)$ and the derivative of $J(\alpha)$ with respect to α is

$$\begin{aligned} \frac{\partial J(\alpha)}{\partial \alpha_k} = & \frac{[\Phi(\alpha_k) - \Phi(\alpha_{k-1})]^2}{(\alpha_k - \alpha_{k-1})^2} - 2 \frac{\Phi(\alpha_k) - \Phi(\alpha_{k-1})}{\alpha_k - \alpha_{k-1}} \phi(\alpha_k) \\ & - \frac{[\Phi(\alpha_{k+1}) - \Phi(\alpha_k)]^2}{(\alpha_{k+1} - \alpha_k)^2} + 2 \frac{\Phi(\alpha_{k+1}) - \Phi(\alpha_k)}{\alpha_{k+1} - \alpha_k} \phi(\alpha_k) \end{aligned} \quad (24)$$

for all $k = 1, \dots, n$. The algorithm is summarized in Algorithm 4.

Algorithm 4 Optimization for Approximating General Spectrum Functions

- 1: Initialize α with $\alpha_0 = 0$, $\alpha_n = 1$ and $\alpha_k \leq \alpha_{k+1}$ for all $k = 1, \dots, n-1$. Set $t \leftarrow 1$.
 - 2: Compute the gradient $\frac{\partial J(\alpha^t)}{\partial \alpha_k}$ using (24).
 - 3: Let $\alpha_k^{t+1} = \alpha_k^t - \theta^t \frac{\partial J(\alpha)}{\partial \alpha_k^t}$ and $\alpha_{(k)}^{t+1}$ be the k -th smallest in set $\{\alpha_k^{t+1} : k = 1, 2, \dots, n\}$. Set $\alpha_k^{t+1} \leftarrow \alpha_{(k)}^{t+1}$ for all k and $t \leftarrow t + 1$. Repeat Step 2 until $\|\alpha^t - \alpha^{t-1}\| \leq \epsilon$.
-

Step 3 guarantees $\alpha_{k-1} \leq \alpha_k$ by sorting $\{\alpha_k : i = 1, 2, \dots, n\}$ in ascending order in each iteration. Note that ϵ is a small positive constant and θ^t is the step size at iteration t . We use the diminishing step size rule for θ^t . When α is obtained, h can be calculated by (23) and ϕ in the optimal step function will be given accordingly. Figure 9 shows an arbitrary step function and the optimal solution to approximate an exponential function with $\sigma = 10^4$ using 3 steps.

6 Numerical Experiments

In this section, applications of the proposed model are shown. We conduct the numerical experiments on the Ravenna (Bonvicini and Spadoni, 2008; Erkut and Gzara, 2008), the Albany (Kang et al., 2014b), the Buffalo (Toumazis and Kwon, 2016) and the Barcelona (Transportation Networks for Research Core Team, 2018) networks. Ravenna is a small town located in Italy where large

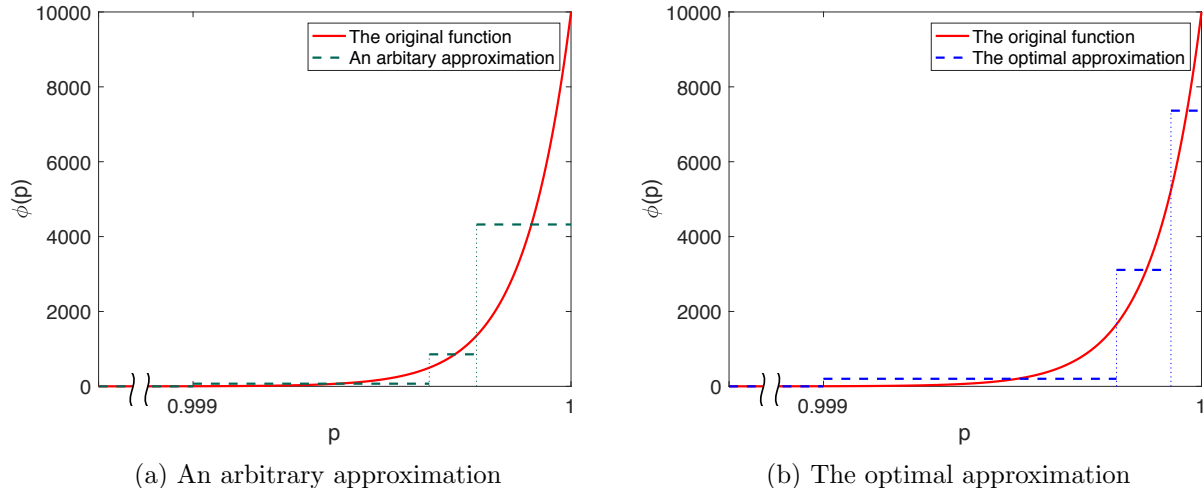


Figure 9: Different approximations for a spectral risk function

amounts of hazardous materials are processed annually. In the Ravenna network, there are 105 nodes and 134 undirected arcs. The data set includes the length, the population that hazmat would influence and the probability of accidents for each arc. The size of Albany and Buffalo networks are similar to Ravenna network. The Barcelona network is large and complicated with 1020 nodes and 2522 directed arcs. For the Barcelona network, accident probabilities and accident consequences are randomly generated.

All computational schemes introduced in this paper are coded in Python. The Gurobi solver version 6.5.1 is used. The experiments are implemented on a 2.2 GHz Xeon processor and 32 GB of RAM.

6.1 Comparisons for Algorithms

To show the performances of the proposed algorithms, the computation time and optimality gap are provided in Table 2. MILP reformulation introduced in Section 4.2 is directly solved by Gurobi while k shortest path approach generates 10,000 candidates to obtain minimal SRM path. With the optimal step function obtained by Algorithm 4, we implement MILP reformulation, Algorithms 2 and 3 for finding a safe path in hazmat transportation. In Table 2, Algorithms 2 and 3 are always more efficient than the k shortest path approach. For small networks such as Buffalo, Ravenna and Albany, Algorithm 2 can still solve the SRM hazmat routing problem efficiently with extremely small or none optimality gaps although MILP reformulation usually performs best in such cases. Algorithms 2 and 3 can be both effective and efficient for the Barcelona network while MILP reformulation and k shortest path are inefficient. Figure 10 shows the computation time for the Barcelona network with various OD pairs. For this large and complicated network, we can see that Algorithm 2 is the most efficient. Algorithm 3 also performs well in most cases.

Detailed comparisons for Algorithms 2 and 3 are conducted on the Ravenna network. The results show that exponential functions and power functions share the same optimal step function

Table 2: Comparisons of different algorithms

| Network | OD pair | σ | Computation time in seconds (optimality gap) | | | | | | | |
|-----------|----------|----------|--|------|-------------------|---------|-------------|---------|-------------|------|
| | | | MILP reformulation | | k shortest path | | Algorithm 2 | | Algorithm 3 | |
| Buffalo | (1,15) | 10^4 | 0.427 | (0%) | 441.890 | (0%) | 5.049 | (0%) | 175.464 | (0%) |
| | | 10^5 | 0.633 | (0%) | 438.998 | (0%) | 9.960 | (0%) | 166.252 | (0%) |
| | | 10^6 | 4.609 | (0%) | 439.000 | (0%) | 22.601 | (2.63%) | 179.742 | (0%) |
| Ravenna | (106,71) | 10^4 | 21.550 | (0%) | 402.870 | (0%) | 16.161 | (0%) | 186.103 | (0%) |
| | | 10^5 | 2.920 | (0%) | 402.789 | (0%) | 10.401 | (0%) | 184.690 | (0%) |
| | | 10^6 | 1.135 | (0%) | 407.712 | (0%) | 10.451 | (3.34%) | 200.474 | (0%) |
| Albany | (1,15) | 10^4 | 0.431 | (0%) | 318.061 | (0%) | 5.064 | (0%) | 150.950 | (0%) |
| | | 10^5 | 1.057 | (0%) | 318.057 | (0%) | 16.100 | (0%) | 147.464 | (0%) |
| | | 10^6 | 0.956 | (0%) | 318.038 | (0%) | 10.380 | (0%) | 158.821 | (0%) |
| Barcelona | (3,600) | 10^4 | 107.204 | (0%) | 7988.353 | (2.18%) | 57.266 | (0%) | 2469.816 | (0%) |
| | | 10^5 | 39321.988 | (0%) | 7985.875 | (6.88%) | 184.726 | (0%) | 2567.690 | (0%) |
| | | 10^6 | 872.329 | (0%) | 7984.812 | (0.98%) | 237.256 | (0%) | 2546.374 | (0%) |

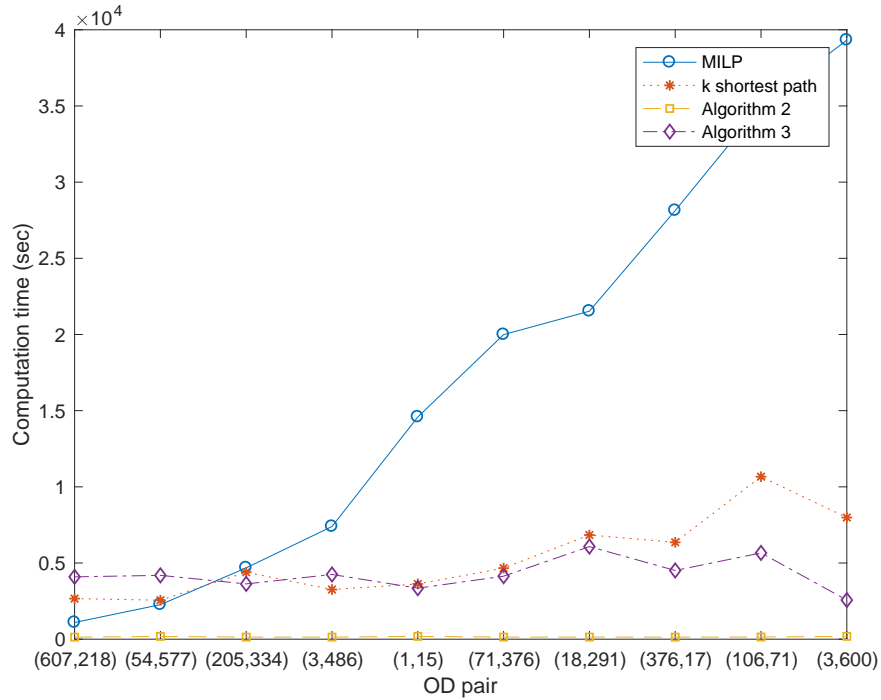
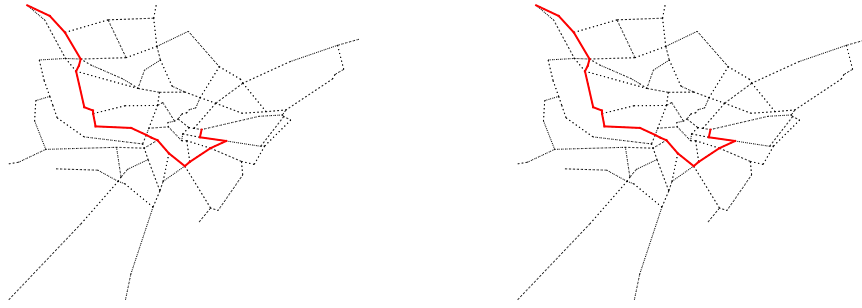
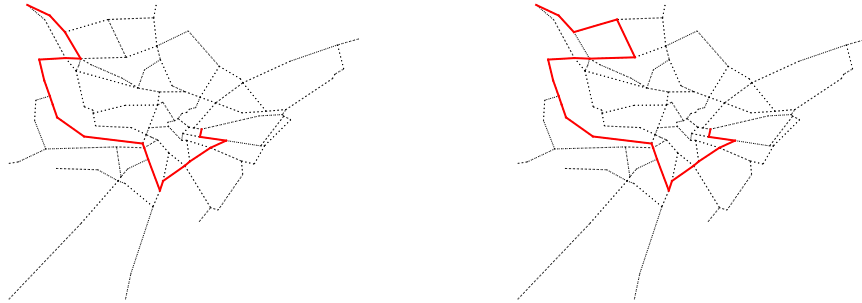


Figure 10: Computation time for various OD pairs with Barcelona network when $\sigma = 10^5$



(a) $\min_{l \in \mathcal{P}} \text{SRM}_\phi^l = 1791.507$ by Algorithm 2 (b) $\min_{l \in \mathcal{P}} \text{SRM}_\phi^l = 1791.507$ by Algorithm 3

Figure 11: Comparisons for Algorithm 2 and Algorithm 3 when $\sigma = \kappa = 10^4$



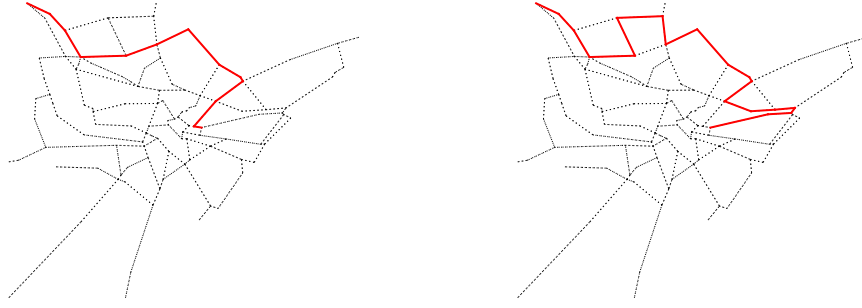
(a) $\min_{l \in \mathcal{P}} \text{SRM}_\phi^l = 2555.770$ by Algorithm 2 (b) $\min_{l \in \mathcal{P}} \text{SRM}_\phi^l = 2555.783$ by Algorithm 3

Figure 12: Comparisons for Algorithm 2 and Algorithm 3 when $\sigma = \kappa = 10^5$

approximations when $\sigma = \kappa$ under the three alternatives. Using node 106 as an origin and node 71 as a destination, the results for the minimal SRM path in hazmat routing are shown in Figures 11, 12, and 13.

Two algorithms can have different performances for different spectral risk measures. In Figure 11, it can be seen that Algorithms 2 and 3 have the same optimal solution when $\sigma = \kappa = 10^4$. With $\sigma = \kappa = 10^5$, Algorithm 2 yields the optimal solution while Algorithm 3 does not. Algorithm 3 provides the optimal solution while Algorithm 2 does not yield the optimal solution if $\sigma = \kappa = 10^6$. A local optimal solution may be found by Algorithm 2 despite a full path set based on the arc-based formulation. On the other hand, Algorithm 3 cannot guarantee the optimal solution because the optimal is chosen from a limited number of path candidates. While there exist some differences in the optimal path solutions, both algorithms obtain similar SRM values.

Both algorithms have their advantages and limitations. If the number of steps for approximation



(a) $\min_{l \in \mathcal{P}} \text{SRM}_\phi^l = 2688.431$ by Algorithm 2 (b) $\min_{l \in \mathcal{P}} \text{SRM}_\phi^l = 2601.665$ by Algorithm 3

Figure 13: Comparisons for Algorithm 2 and Algorithm 3 when $\sigma = \kappa = 10^6$

is very small, Algorithm 2 is recommended. Although losing accuracy in the objective function, the arc-based formulation in Algorithm 2 explores all feasible paths while CVaR path generation in Algorithm 3 produces only a few dissimilar paths when n is small. Algorithm 2 is inefficient if the spectrum function involves a large n . In addition, it can terminate at some local optimal solutions by Algorithm 1 given too many steps of $\phi(\cdot)$. Algorithm 3 is recommended with a large number of steps due to its linear computation complexity in n . Both algorithms can be implemented when a reasonable number of steps is chosen to approximate the general $\phi(\cdot)$.

6.2 Comparisons of Risk Measures and Limitation of CVaR

In the existing literature for hazmat transportation, there are various risk measures including TR, MM and CVaR. Table 3 shows a comparison of paths produced by different models in the Ravenna network. We can find that only the CVaR model with confidence level of 0.999999 and the SRM minimization model with $\sigma = 10^6$ generate the same path; i.e., $l_3 = l_6$. The CVaR model with extremely high confidence levels and the SRM model with very large parameters are equivalent because they only consider MM. Here, the MM path is different from CVaR and SRM paths with extremely large parameters due to multiple optimal solutions aiming at MM.

Table 3: Comparisons of paths for different models in the Ravenna network. Optimal path names are arbitrarily given for convenient explanation.

| Model | | Optimal Path |
|-------|-----------------|---|
| TR | l_{TR} | 106 → 1 → 2 → 7 → 17 → 19 → 28 → 34 → 39 → 47 → 55 → 52 → 53 → 48 → 51 → 63 → 67 → 71 |
| MM | l_{MM} | 106 → 1 → 2 → 4 → 17 → 19 → 23 → 40 → 59 → 64 → 61 → 102 → 82 → 84 → 103 → 81 → 71 |
| CVaR | 0.9999 | l_1 106 → 1 → 2 → 7 → 5 → 10 → 20 → 24 → 26 → 30 → 36 → 43 → 46 → 56 → 69 → 76 → 75 → 77 → 80 → 73 → 71 |
| | 0.999999 | l_2 106 → 1 → 2 → 4 → 17 → 7 → 5 → 3 → 6 → 11 → 14 → 98 → 31 → 45 → 54 → 62 → 78 → 74 → 76 → 75 → 77 → 80 → 73 → 71 |
| | 0.9999999 | l_3 106 → 1 → 2 → 7 → 17 → 4 → 13 → 19 → 23 → 40 → 59 → 64 → 61 → 102 → 82 → 84 → 103 → 81 → 71 |
| SRM | 10^4 | l_4 106 → 1 → 2 → 7 → 9 → 10 → 20 → 24 → 26 → 30 → 36 → 43 → 46 → 56 → 69 → 76 → 75 → 77 → 80 → 73 → 71 |
| | 10^5 | l_5 106 → 1 → 2 → 7 → 5 → 3 → 6 → 11 → 14 → 98 → 31 → 45 → 54 → 62 → 78 → 74 → 76 → 75 → 77 → 80 → 73 → 71 |
| | 10^6 | $l_6 = l_3$ 106 → 1 → 2 → 7 → 17 → 4 → 13 → 19 → 23 → 40 → 59 → 64 → 61 → 102 → 82 → 84 → 103 → 81 → 71 |

Table 4: Comparisons of various risk measures for different models in the Ravenna network.

| Model | Optimal Path l | TR ^{l} ($\times 10^{-4}$) | MM ^{l} | CVaR ^{l} _{α} | | | SRM ^{l} _{σ} | | | # of arcs | length |
|-------|-----------------------------|--|------------------------------|---|-------------|-------------|--|-----------------|-----------------|-----------|--------|
| | | | | 0.9999 | 0.99999 | 0.999999 | 10 ⁴ | 10 ⁵ | 10 ⁶ | | |
| TR | l_{TR} | 4.07 | 5.23 | 2.32 | 3.85 | 5.23 | 1.95 | 3.60 | 5.19 | 17 | 24.33 |
| MM | l_{MM} | 6.28 | 2.60 | 2.22 | 2.60 | 2.60 | 2.05 | 2.56 | 2.60 | 16 | 39.36 |
| CVaR | 0.9999 l_1 | 4.30 | 3.47 | 2.07 | 3.47 | 3.47 | 1.81 | 3.15 | 3.47 | 20 | 30.15 |
| | 0.99999 l_2 | 5.58 | 2.69 | 2.23 | 2.59 | 2.69 | 1.92 | 2.56 | 2.69 | 23 | 45.68 |
| | 0.999999 l_3 | 7.62 | 2.60 | 2.27 | 2.60 | 2.60 | 2.14 | 2.56 | 2.60 | 18 | 45.58 |
| SRM | 10 ⁴ l_4 | 4.10 | 3.47 | 2.07 | 3.47 | 3.47 | 1.79 | 3.15 | 3.47 | 20 | 28.64 |
| | 10 ⁵ l_5 | 4.93 | 2.69 | 2.23 | 2.59 | 2.69 | 1.89 | 2.56 | 2.69 | 21 | 37.32 |
| | 10 ⁶ $l_6 = l_3$ | 7.62 | 2.60 | 2.27 | 2.60 | 2.60 | 2.14 | 2.56 | 2.60 | 18 | 45.58 |

For the Ravenna network, Table 4 compares TR, MM, CVaR and SRM models with respect to various risk measures, the number of arcs and the length of the path. We can re-confirm the limitation of CVaR, observed in the small example in Section 2.2, from the results in Table 4. For the minimization problem with CVaR_{0.9999}, path l_1 is chosen by algorithm, although l_4 also is an optimal solution for the same problem. Path l_4 , however, has not only a smaller TR measure value, but also a shorter length than l_1 . When SRM model with $\sigma = 10^4$ is used, l_4 is chosen. Similarly, we can also compare l_2 and l_5 . While both l_2 and l_5 have the same CVaR_{0.99999} value, path l_5 has smaller TR measure value and shorter length.

When l_1 and l_4 are compared, the only difference is that l_1 utilizes link $7 \rightarrow 5 \rightarrow 10$, while l_4 uses link $7 \rightarrow 9 \rightarrow 10$. In these two subpaths, the accident probability and the accident consequence in each link are shown below:

| | (7, 5) | (5, 10) | (7, 9) | (9, 10) |
|--------------------------|--------|---------|--------|---------|
| $p_{ij}(\times 10^{-5})$ | 1.23 | 1.42 | 0.61 | 0.54 |
| c_{ij} | 1.13 | 1.42 | 1.54 | 0.87 |

Note that in both l_1 and l_4 , we have $\text{VaR}_{0.9999} = 1.57$. In the evaluation fo CVaR_{0.9999}, any link consequence that is smaller than $\text{VaR}_{0.9999}$ is cut off, or ignored, as we can see from Theorem 5—note $\mathbb{E}[X - r]^+$ in (25). Therefore, all four above links have no impact on CVaR_{0.9999}. However, we should note that the risk in $7 \rightarrow 9 \rightarrow 10$ has the smaller expected value than in $7 \rightarrow 5 \rightarrow 10$; hence l_4 should be preferred to l_1 .

Similarly, when l_2 and l_5 are compared, the only difference is that l_2 utilizes link $2 \rightarrow 4 \rightarrow 17 \rightarrow 7$, while l_5 directly moves $2 \rightarrow 7$. The probabilities and consequences respectively are

| | (2, 4) | (4, 17) | (17, 7) |
|--------------------------|--------|---------|---------|
| $p_{ij}(\times 10^{-5})$ | 3.68 | 3.65 | 3.70 |
| c_{ij} | 0.58 | 1.88 | 0.69 |

Since $\text{VaR}_{0.99999} = 2.46$ in path l_2 , all above three links are cut off in computing CVaR_{0.99999}. Hence,

Table 5: Multiple optimal paths for $\text{CVaR}_{0.999995}$ in the Barcelona network for OD pair (3, 600). Optimal path names are arbitrarily given for convenient explanation.

| Model | Optimal Path l | TR^l | $\text{VaR}_{0.999995}^l$ | $\text{CVaR}_{0.999995}^l$ | # of arcs |
|-------|------------------|---------------|---------------------------|----------------------------|-----------|
| CVaR | l_1^B | 0.0312 | 1.7473 | 3.4831 | 60 |
| | l_2^B | 0.0310 | 1.7473 | 3.4831 | 61 |
| | l_3^B | 0.0311 | 1.7473 | 3.4831 | 60 |
| | l_4^B | 0.0309 | 1.7473 | 3.4831 | 61 |
| | l_5^B | 0.0309 | 1.7473 | 3.4831 | 61 |
| | l_6^B | 0.0312 | 1.7473 | 3.4831 | 60 |
| | l_7^B | 0.0299 | 1.7473 | 3.4831 | 64 |
| SRM | l_8^B | 0.0297 | 1.7473 | 3.4831 | 65 |

in the shortest-path sub-problem to compute $\text{CVaR}_{0.99999}$, these three links are regarded as links with zero link costs. It is evident, however, that l_5 must be preferred to l_2 .

The paths in Table 5 are shown in Table 6 in the appendix. We find multiple optimal $\text{CVaR}_{0.999995}$ paths while SRM model can directly find l_8^B with a two-step spectrum function for $\alpha_2 = 0.999995$ and some $0 < \phi_1 < 1, \phi_2 = 2 \cdot 10^5(1 - \phi_1)$. Note that the SRM model is equivalent to CVaR model when $\phi_1 = 0$. Given $\phi_1 > 0$, the SRM model here considers the minimum weight average of TR and CVaR. The eight CVaR paths have significant differences in TR values among which the minimum TR path is obtained by SRM model. For large-scale networks like Barcelona, it is possible that there exist multiple optimal CVaR paths. CVaR model, however, cannot distinguish those paths in terms of other measures of interest. With proper SRM parameters, we can use the proposed model to find the path with both minimal CVaR value and minimal TR value.

As it is demonstrated in the above cases, SRM is obviously a better decision model than CVaR, although CVaR provides a flexible tool for risk-averse hazmat routing.

7 Concluding Remarks

To make risk-averse decisions, we consider spectral risk measures, which are coherent and more general than other well-known risk measures such as conditional value-at-risk. In the context of hazmat transportation, we apply spectral risk measures to the routing problem. We propose the SRM minimization model for a safe path and develop an efficient algorithm for a special class of spectral risk measures. For the general spectral risk measures, it is difficult to transform the path-based formulation to an arc-based formulation. Hence, we propose two algorithms for general spectral risk routing problems. In addition, various spectrum functions are discussed to provide some guidance for generating safe paths in hazmat transportation. The performance of algorithms are compared for various networks to show the effectiveness and efficiency of the proposed methods. The two algorithms to obtain the general minimal SRM path are also compared in different cases. In some situations, there exist differences in the optimal routing between the two algorithms, however

their spectral risk measures are very close.

Through numerical examples, we have demonstrated the cases when CVaR minimization provides less desirable solutions. Often there are multiple least CVaR paths, since CVaR cuts off links whose accident consequences are smaller than VaR. In such case, CVaR minimization algorithms can find a path with greater expected risk values, which must be avoided. We demonstrated that SRM can be a solution for such cases.

Although SRM demonstrate desirable properties, there still exists a limitation. In most cases, it is unclear how the spectrum function or parameters in a spectrum function should be determined. As in Theorem 2, we can define a special SRM as a weighted average of three popular risk measures, namely, TR, CVaR, and MM. When a proper choice of the spectrum function is vague, such a weighted average can serve a practical way of determining a safe route for hazmat transportation.

We propose a few avenues for future research. First, we can consider the uncertainty of data associated with risk in hazmat routing. Since there exist few accident statistics for hazmat transportation, we can incorporate data uncertainty into spectral risk measures to obtain safe paths. Second, a network design problem addressing spectral risks can be developed. In this design problem, decision makers can introduce a road banning policy or a road pricing policy to minimize the system-wide spectral risk measure value by considering routing behavior of hazmat carriers via bilevel optimization as in Stackelberg games. Third, we can apply SRM to other transportation problems. Since CVaR or related concepts, such as mean-excess measures, have been applied in other areas of transportation (Chen and Zhou, 2010; Chen et al., 2006; Soleimani and Govindan, 2014), it will be worth studying the shortcomings of CVaR in other applications and how SRM can be utilized.

Acknowledgments This research was supported by the National Science Foundation grant CMMI-1558359.

Appendix

We need the following theorem for proofs:

Theorem 5 (Rockafellar and Uryasev, 2002). *For $r \in \mathbb{R}$, let us define*

$$F_\alpha(r; X) = r + \frac{1}{1-\alpha} \mathbb{E}[X - r]^+, \quad (25)$$

where $[x]^+ = \max(x, 0)$. Then the CVaR measure is equivalent to:

$$\text{CVaR}_\alpha(X) = \min_{r \in \mathbb{R}} F_\alpha(r; X) \quad (26)$$

and

$$\text{VaR}_\alpha(X) = \arg \min_{r \in \mathbb{R}} F_\alpha(r; X). \quad (27)$$

We provide proofs for lemmas and theorems as follows:

Proof of Lemma 1. Note that

$$\begin{aligned}
& \int_0^1 \phi(p) dp \\
&= \int_{\alpha_1}^{\alpha_2} \phi_1 dp + \int_{\alpha_2}^{\alpha_3} (\phi_1 + \phi_2) dp + \int_{\alpha_3}^{\alpha_4} (\phi_1 + \phi_2 + \phi_3) dp + \cdots + \int_{\alpha_n}^1 (\phi_1 + \phi_2 + \cdots + \phi_n) dp \\
&= \phi_1(\alpha_2 - \alpha_1) + (\phi_1 + \phi_2)(\alpha_3 - \alpha_2) + (\phi_1 + \phi_2 + \phi_3)(\alpha_4 - \alpha_3) + \cdots + (\phi_1 + \phi_2 + \cdots + \phi_n)(1 - \alpha_n) \\
&= \phi_1(1 - \alpha_1) + \phi_2(1 - \alpha_2) + \cdots + \phi_n(1 - \alpha_n) \\
&= \sum_{k=1}^n \phi_k(1 - \alpha_k).
\end{aligned}$$

From the normalization condition (7), we obtain the lemma. \square

Proof of Theorem 1. From Definition 3, we have

$$\begin{aligned}
\text{SRM}_\phi^l &= \int_0^1 \phi(p) \text{VaR}_p^l dp \\
&= \phi_0 \int_0^1 \text{VaR}_p^l dp + \phi_1 \int_{\alpha_1}^1 \text{VaR}_p^l dp + \phi_2 \int_{\alpha_2}^1 \text{VaR}_p^l dp + \cdots + \phi_n \int_{\alpha_n}^1 \text{VaR}_p^l dp \\
&= \sum_{k=1}^n \phi_k(1 - \alpha_k) \text{CVaR}_{\alpha_k}^l
\end{aligned}$$

where we use the definition of CVaR in (4). Note that $\text{CVaR}_{\alpha_1}^l$ is $\mathbb{E}[R^l]$. Theorem 5 yields (10). \square

Proof of Theorem 2. From Theorems 1 and 2 of Toumazis and Kwon (2013), we have

$$\begin{aligned}
\Sigma^l &= w_1 \text{TR}^l + w_2 \text{CVaR}_\alpha^l + w_3 \text{MM}^l \\
&= w_1 \mathbb{E}[R^l] + w_2 \text{CVaR}_\alpha^l + w_3 \sup R^l \\
&= w_1 \text{CVaR}_{\alpha_1}^l + w_2 \text{CVaR}_\alpha^l + w_3 \text{CVaR}_{\alpha_3}^l
\end{aligned}$$

where $\alpha_1 = 0$ and $\alpha_3 = p^l$. By Theorem 1, we have a proof. \square

Proof of Theorem 3. We have

$$\begin{aligned}
\min_{l \in \mathcal{P}} \text{SRM}_\phi^l &= \min_{l \in \mathcal{P}} \sum_{k=1}^n \phi_k(1 - \alpha_k) \min_{r_k} \left[r_k + \frac{1}{1 - \alpha_k} \sum_{(i,j) \in \mathcal{A}^l} p_{ij} [c_{ij} - r_k]^+ \right] \\
&= \min_{x \in \Omega} \sum_{k=1}^n \phi_k(1 - \alpha_k) \min_{r_k} \left[r_k + \frac{1}{1 - \alpha_k} \sum_{(i,j) \in \mathcal{A}} p_{ij} [c_{ij} - r_k]^+ x_{ij} \right] \\
&= \min_{x \in \Omega} \sum_{k=1}^n \min_{r_k} \phi_k(1 - \alpha_k) \left[r_k + \frac{1}{1 - \alpha_k} \sum_{(i,j) \in \mathcal{A}} p_{ij} [c_{ij} - r_k]^+ x_{ij} \right]
\end{aligned}$$

$$= \min_{x \in \Omega} \sum_{k=1}^n \min_{r_k} f_k(r_k, x)$$

where

$$f_k(r_k, x) \equiv \phi_k(1 - \alpha_k) \left[r_k + \frac{1}{1 - \alpha_k} \sum_{(i,j) \in \mathcal{A}} p_{ij} [c_{ij} - r_k]^+ x_{ij} \right]$$

We note that $f_k(r_k, x)$ is independent from r_j for all $j \neq k$. Therefore, introducing a vector notation $r = [r_1, \dots, r_n]^T$, we can write:

$$\begin{aligned} \min_{l \in \mathcal{P}} \text{SRM}_\phi^l &= \min_{x \in \Omega} \min_r \sum_{k=1}^n f_k(r_k, x) \\ &= \min_{x \in \Omega} \min_r \sum_{k=1}^n \phi_k(1 - \alpha_k) \left[r_k + \frac{1}{1 - \alpha_k} \sum_{(i,j) \in \mathcal{A}} p_{ij} [c_{ij} - r_k]^+ x_{ij} \right] \\ &= \min_{x \in \Omega} \min_r \left[\sum_{k=1}^n \phi_k(1 - \alpha_k) r_k + \sum_{k=1}^n \phi_k \sum_{(i,j) \in \mathcal{A}} p_{ij} [c_{ij} - r_k]^+ x_{ij} \right] \\ &= \min_r \left[\sum_{k=1}^n \phi_k(1 - \alpha_k) r_k + \min_{x \in \Omega} \sum_{(i,j) \in \mathcal{A}} \left\{ \sum_{k=1}^n \phi_k p_{ij} [c_{ij} - r_k]^+ \right\} x_{ij} \right] \end{aligned} \quad (28)$$

When r is a given vector, we can solve the inner problem as a shortest-path problem with the cost in each arc (i, j) as $\sum_{k=1}^n \phi_k p_{ij} [c_{ij} - r_k]^+$. \square

Proof of Lemma 3. By letting $r^{\alpha_1} = \text{VaR}_{\alpha_1}^l$ and $r^{\alpha_2} = \text{VaR}_{\alpha_2}^l$, the lemma is immediate from Definition 1. \square

Proof of Theorem 4. We rewrite (19) as follows:

$$E(\alpha, h) = \sum_{k=1}^n \left[\int_{\alpha_{k-1}}^{\alpha_k} \{\phi(p)\}^2 dp - 2h_k \int_{\alpha_{k-1}}^{\alpha_k} \phi(p) dp + h_k^2 (\alpha_k - \alpha_{k-1}) \right]. \quad (29)$$

For any given α_k values, we note that

$$\frac{\partial E}{\partial h_k} = -2 \int_{\alpha_{k-1}}^{\alpha_k} \phi(p) dp + 2h_k (\alpha_k - \alpha_{k-1}), \quad (30)$$

$$\frac{\partial^2 E}{\partial h_k^2} = 2(\alpha_k - \alpha_{k-1}) \geq 0 \quad (31)$$

for all $k = 1, \dots, n$. Thus, $E(\alpha, h)$ is convex with respect to h_k , for any given α_k values. Letting $\frac{\partial E}{\partial h_k} = 0$, we obtain

$$h_k = \frac{\int_{\alpha_{k-1}}^{\alpha_k} \phi(p) dp}{\alpha_k - \alpha_{k-1}} = \frac{\Phi(\alpha_k) - \Phi(\alpha_{k-1})}{\alpha_k - \alpha_{k-1}} \quad (32)$$

for all $k = 1, \dots, n$. Besides, $\sum_{k=1}^n h_k (\alpha_k - \alpha_{k-1}) = \int_0^1 \phi(p) dp = 1$ satisfies (20) automatically.

Using (32) in (29), we obtain

$$\begin{aligned}
& \sum_{k=1}^n \left[\int_{\alpha_{k-1}}^{\alpha_k} \{\phi(p)\}^2 dp - \frac{[\Phi(\alpha_k) - \Phi(\alpha_{k-1})]^2}{\alpha_k - \alpha_{k-1}} \right] \\
&= \sum_{k=1}^n \int_{\alpha_{k-1}}^{\alpha_k} \{\phi(p)\}^2 dp - \sum_{k=1}^n \frac{[\Phi(\alpha_k) - \Phi(\alpha_{k-1})]^2}{\alpha_k - \alpha_{k-1}} \\
&= \int_0^1 \{\phi(p)\}^2 dp - \sum_{k=1}^n \frac{[\Phi(\alpha_k) - \Phi(\alpha_{k-1})]^2}{\alpha_k - \alpha_{k-1}} \tag{33}
\end{aligned}$$

Since $\int_0^1 \{\phi(p)\}^2 dp$ is a constant, we obtain the theorem. □

Table 6: Paths in Table 5

| | |
|---------|--|
| l_1^B | {3, 306, 308, 307, 312, 305, 313, 90, 322, 318, 332, 851, 846, 841, 317, 27, 824, 825, 328, 320, 329, 339, 448, 338, 364, 779, 787, 769, 772, 810, 773, 796, 815, 802, 348, 444, 349, 395, 396, 464, 459, 453, 468, 483, 205, 206, 486, 545, 547, 532, 533, 15, 538, 539, 226, 235, 236, 602, 605, 593, 600} |
| l_2^B | {3, 306, 308, 307, 312, 305, 313, 90, 322, 318, 332, 851, 846, 841, 317, 27, 824, 825, 328, 320, 329, 339, 448, 338, 364, 779, 787, 769, 772, 810, 773, 796, 815, 802, 348, 444, 349, 395, 396, 464, 459, 453, 468, 483, 205, 206, 486, 545, 547, 532, 533, 15, 538, 539, 226, 235, 236, 602, 603, 606, 593, 600} |
| l_3^B | {3, 306, 308, 307, 312, 305, 313, 90, 322, 318, 332, 851, 846, 841, 317, 27, 824, 825, 328, 320, 329, 339, 448, 338, 364, 779, 783, 768, 790, 794, 809, 800, 388, 442, 443, 444, 349, 395, 396, 464, 459, 453, 468, 483, 205, 206, 486, 545, 547, 532, 533, 15, 538, 539, 226, 235, 236, 602, 605, 593, 600} |
| l_4^B | {3, 306, 308, 307, 312, 305, 313, 90, 322, 318, 332, 851, 846, 841, 317, 27, 824, 825, 328, 320, 329, 339, 448, 338, 364, 779, 783, 768, 790, 794, 809, 800, 388, 442, 443, 444, 349, 395, 396, 464, 459, 453, 468, 483, 205, 206, 486, 545, 547, 532, 533, 15, 538, 539, 226, 235, 236, 602, 603, 606, 593, 600} |
| l_5^B | {3, 306, 308, 307, 312, 305, 313, 90, 322, 318, 332, 851, 846, 841, 317, 27, 824, 825, 328, 320, 329, 339, 448, 338, 364, 779, 787, 788, 790, 794, 809, 800, 388, 442, 443, 444, 349, 395, 396, 464, 459, 453, 468, 483, 205, 206, 486, 545, 547, 532, 533, 15, 538, 539, 226, 235, 236, 602, 603, 606, 593, 600} |
| l_6^B | {3, 306, 308, 307, 312, 305, 313, 90, 322, 318, 332, 851, 846, 841, 317, 27, 824, 825, 328, 320, 329, 339, 448, 338, 364, 779, 787, 788, 790, 794, 809, 800, 388, 442, 443, 444, 349, 395, 396, 464, 459, 453, 468, 483, 205, 206, 486, 545, 547, 532, 533, 15, 538, 539, 226, 235, 236, 602, 605, 593, 600} |
| l_7^B | {3, 306, 308, 307, 312, 305, 313, 90, 322, 318, 332, 851, 846, 841, 317, 27, 824, 825, 328, 320, 329, 339, 448, 338, 364, 779, 787, 769, 772, 767, 791, 764, 780, 812, 798, 804, 458, 505, 451, 495, 511, 453, 475, 454, 455, 471, 476, 568, 530, 523, 581, 580, 578, 575, 240, 241, 538, 539, 226, 235, 236, 602, 605, 593, 600} |
| l_8^B | {3, 306, 308, 307, 312, 305, 313, 90, 322, 318, 332, 851, 846, 841, 317, 27, 824, 825, 328, 320, 329, 339, 448, 338, 364, 779, 787, 769, 772, 767, 791, 764, 780, 812, 798, 804, 458, 505, 451, 495, 511, 453, 475, 454, 455, 471, 476, 568, 530, 523, 581, 580, 578, 575, 240, 241, 538, 539, 226, 235, 236, 602, 603, 606, 593, 600} |

References

- Abkowitz, M., M. Lepofsky, P. Cheng. 1992. Selecting criteria for designating hazardous materials highway routes. *Transportation Research Record* **1333** 30–35.
- Acerbi, C. 2002. Spectral measures of risk: a coherent representation of subjective risk aversion. *Journal of Banking & Finance* **26**(7) 1505–1518.
- Acerbi, C. 2004. Coherent representations of subjective risk-aversion. G. Szeö, ed., *Risk Measures for the 21st Century*. New York: Wiley, 147–207.

- Acerbi, C., D. Tasche. 2002. On the coherence of expected shortfall. *Journal of Banking & Finance* **26**(7) 1487–1503.
- Acerbi, C., P. Simonetti. 2008. Portfolio optimization with spectral measures of risk. URL <http://arxiv.org/abs/cond-mat/0203607>. <http://arxiv.org/abs/cond-mat/0203607>.
- Akgün, V., E. Erkut, R. Batta. 2000. On finding dissimilar paths. *European Journal of Operational Research* **121**(2) 232–246.
- Alp, E. 1995. Risk-based transportation planning practice: overall methodology and a case example. *INFOR* **33**(1) 4–19.
- Artzner, P., F. Delbaen, J. Eber, D. Heath. 1999. Coherent measures of risk. *Mathematical Finance* **9**(3) 203–228.
- Bonvicini, S., G. Spadoni. 2008. A hazmat multi-commodity routing model satisfying risk criteria: a case study. *Journal of Loss Prevention in the Process Industries* **21**(4) 345–358.
- Brandtner, M. 2016. Spectral risk measures: Properties and limitations: comment on Dowd, Cotter, and Sorwar. *Journal of Financial Services Research* **49**(1) 121–131.
- Brandtner, M., W. Kürsten. 2017. Consistent modeling of risk averse behavior with spectral risk measures: Wächter/Mazzoni revisited. *European Journal of Operational Research* **259**(1) 394–399.
- Chen, A., Z. Zhou. 2010. The α -reliable mean-excess traffic equilibrium model with stochastic travel times. *Transportation Research Part B* **44** 493–513.
- Chen, G., M. S. Daskin, Z.-J. M. Shen, S. Uryasev. 2006. The α -reliable mean-excess regret model for stochastic facility location modeling. *Wiley Periodicals, Inc. Naval Research Logistics* **53** 617–626.
- Dowd, K., D. Blake. 2006. After VaR: the theory, estimation, and insurance applications of quantile-based risk measures. *Journal of Risk and Insurance* **73**(2) 193–229.
- Dowd, K., J. Cotter, G. Sorwar. 2008. Spectral risk measures: properties and limitations. *Journal of Financial Services Research* **34**(1) 61–75.
- Erkut, E., A. Ingolfsson. 2000. Catastrophe avoidance models for hazardous materials route planning. *Transportation Science* **34**(2) 165–179.
- Erkut, E., V. Verter. 1998. Modeling of transport risk for hazardous materials. *Operations Research* **46**(5) 625–642.
- Erkut, E., F. Gzara. 2008. Solving the hazmat transport network design problem. *Computers & Operations Research* **35**(7) 2234–2247.

- Erkut, E., A. Ingolfsson. 2005. Transport risk models for hazardous materials: revisited. *Operations Research Letters* **33**(1) 81–89.
- Erkut, E., S. A. Tjandra, V. Verter. 2007. Hazardous materials transportation. *Handbooks in Operations Research & Management Science* **14** 539–621.
- Hosseini, S. D., M. Verma. 2018. Conditional value-at-risk (CVaR) methodology to optimal train configuration and routing of rail hazmat shipments. *Transportation Research Part B: Methodological* **110** 79–103.
- Jin, H., R. Batta. 1997. Objectives derived from viewing hazmat shipments as a sequence of independent bernoulli trials. *Transportation Science* **31**(3) 252–261.
- Kang, Y., R. Batta, C. Kwon. 2014a. Generalized route planning model for hazardous material transportation with VaR and equity considerations. *Computers & Operations Research* **43** 237–247.
- Kang, Y., R. Batta, C. Kwon. 2014b. Value-at-risk model for hazardous material transportation. *Annals of Operations Research* **222**(1) 361–387.
- Marhavilas, P.-K., D. Koulouriotis, V. Gemeni. 2011. Risk analysis and assessment methodologies in the work sites: on a review, classification and comparative study of the scientific literature of the period 2000–2009. *Journal of Loss Prevention in the Process Industries* **24**(5) 477–523.
- Maybee, J., P. Randolph, N. Uri. 1979. Optimal step function approximations to utility load duration curves. *Engineering Optimization* **4**(2) 89–93.
- Occupational Safety and Health Administration. 2017. Chemical hazards and toxic substances. URL <https://www.osha.gov/SLTC/hazardoustoxicsubstances/index.html>.
- Oggero, A., R. Darbra, M. Munoz, E. Planas, J. Casal. 2006. A survey of accidents occurring during the transport of hazardous substances by road and rail. *Journal of Hazardous Materials* **133**(1-3) 1–7.
- Pflug, G. 2000. Some remarks on the value-at-risk and the conditional value-at-risk. S. P. Uryasev, ed., *Probabilistic Constrained Optimization: Methodology and Applications, Nonconvex Optimization and Its Applications*, vol. 38. Kluwer Academic Publishers, Dordrecht, The Netherlands, 272–281.
- Pipeline and Hazardous Materials Safety Administration. 2017. Incident statistics. URL <https://www.phmsa.dot.gov/hazmat/library/data-stats/incidents>.
- Rayas, V. M., M. A. Serrato. 2017. A framework of the risk assessment for the supply chain of hazardous materials. *Netnomics: Economic Research and Electronic Networking* **18**(2-3) 215–226.

- ReVelle, C., J. Cohon, D. Shobrys. 1991. Simultaneous siting and routing in the disposal of hazardous wastes. *Transportation Science* **25**(2) 138–145.
- Rockafellar, R., S. Uryasev. 2002. Conditional value-at-risk for general loss distributions. *Journal of Banking & Finance* **26**(7) 1443–1471.
- Saccomanno, F., A. Chan. 1985. Economic evaluation of routing strategies for hazardous road shipments. *Transportation Research Record* **1020** 12–18.
- Sivakumar, R. A., B. Rajan, M. Karwan. 1993. A network-based model for transporting extremely hazardous materials. *Operations Research Letters* **13**(2) 85–93.
- Soleimani, H., K. Govindan. 2014. Reverse logistics network design and planning utilizing conditional value at risk. *European Journal of Operational Research* **237**(2) 487–497.
- Tomasoni, A. M., E. Garbolino, M. Rovatti, R. Sacile. 2010. Risk evaluation of real-time accident scenarios in the transport of hazardous material on road. *Management of Environmental Quality: An International Journal* **21**(5) 695–711.
- Torretta, V., E. C. Rada, M. Schiavon, P. Viotti. 2017. Decision support systems for assessing risks involved in transporting hazardous materials: a review. *Safety Science* **92** 1–9.
- Toumazis, I., C. Kwon. 2013. Routing hazardous materials on time-dependent networks using conditional value-at-risk. *Transportation Research Part C: Emerging Technologies* **37** 73–92.
- Toumazis, I., C. Kwon. 2016. Worst-case conditional value-at-risk minimization for hazardous materials transportation. *Transportation Science* **50**(4) 1174–1187. doi:10.1287/trsc.2015.0639. URL <http://dx.doi.org/10.1287/trsc.2015.0639>.
- Toumazis, I., C. Kwon, R. Batta. 2013. Value-at-risk and conditional value-at-risk minimization for hazardous materials routing. R. Batta, C. Kwon, eds., *Handbook of OR/MS Models in Hazardous Materials Transportation*. Springer.
- Transportation Networks for Research Core Team. 2018. Transportation networks for research. URL <https://github.com/bstabler/TransportationNetworks>. Last Accessed on February 22, 2018.
- Van Raemdonck, K., C. Macharis, O. Mairesse. 2013. Risk analysis system for the transport of hazardous materials. *Journal of Safety Research* **45** 55–63.
- Wächter, H. P., T. Mazzoni. 2013. Consistent modeling of risk averse behavior with spectral risk measures. *European Journal of Operational Research* **229**(2) 487–495.
- Woodruff, J. M. 2005. Consequence and likelihood in risk estimation: a matter of balance in UK health and safety risk assessment practice. *Safety Science* **43**(5-6) 345–353.

Yang, J., F. Li, J. Zhou, L. Zhang, L. Huang, J. Bi. 2010. A survey on hazardous materials accidents during road transport in China from 2000 to 2008. *Journal of Hazardous Materials* **184**(1-3) 647–653.